Role of sticky interstellar organic material in the formation of asteroids

T. Kudo, A. Kouchi, M. Arakawa and H. Nakano

Institute of Low Temperature Science, Hokkaido University, Sapporo 060-0819, Japan

Abstract

Collision experiments and measurements of viscoelastic properties were performed involving an interstellar organic material analogue to investigate the growth of organic grains in the protosolar nebula. The organic material was found to be stickiest at a radius of between 2.3 and 3.0 AU, with a maximum sticking velocity of 5 m s^{-1} for millimeter-size organic grains. This stickiness is considered to have resulted in the very rapid coagulation of organic grain aggregates and subsequent formation of planetesimals in the early stage of the turbulent accretion disk. The planetesimals formed in this region appear to be represent achondrite parent bodies. In contrast, the formation of planetesimals at <2.1 AU and >3.0 AU begins with the establishment of a passive disk because silicate and ice grains are not as sticky as organic grains.

INTRODUCTION

Interstellar grains in molecular clouds consist of silicate minerals, organic material, and ices (Greenberg, 1998). These interstellar grains are heated and partially evaporated (evaporation metamorphism) during the birth of the protosolar nebula, and the remaining core-mantle grains grow into large aggregates by collision and subsequent sticking.

It is important to investigate the heating of interstellar organic

grains to discuss the distribution of planetary material in the protosolar nebula. Although heating experiments have already been performed using silicates (e.g., Hashimoto et al., 1979) and ices (e.g., Bar-Nun et al., 1995; Kouchi, 1990) in a vacuum, experiments involving organic material have not been attempted. Therefore, the present authors recently performed heating experiments on an analogue of interstellar organic matter using chemical reagents (Kouchi et al., 2002; Nakano et al., 2002).

For planetesimals to grow in the protosolar nebula, dust grains and aggregates thereof must coagulate by collision and sticking (Weidenschilling and Cuzzi, 1993). Although a number of theoretical studies have been performed on the coagulation of solid particles (e.g., Chokshi et al., 1993; Dominik and Tielens, 1997; Sirono, 1999), the exact sticking mechanisms involved remain unclear. Collision experiments have been carried out for silicates (e.g., Hartmann, 1978; Blum and Muench, 1993; Wurm and Blum, 1998; Poppe et al., 2000) and ice grains (e.g., Bridges et al., 1984; Hatzes et al., 1988; Higa et al., 1998), but not for organic material. The present authors therefore performed collision experiments involving organic matter in order to understand the effects of organic matter on the coagulation of dust grains (Kouchi et al., 2002).

In the present paper, recent collision experiments and measurements of the viscoelastic properties of organic material are reported, and based on the results and results of previous heating experiments (Kouchi et al., 2002; Nakano et al. 2002), the origin of asteroids and meteorites is discussed.

EXPERIMENTAL

Starting materials

Analogue of interstellar organic matter were prepared by mixing chemical reagents according to the method described in Kouchi et al. (2002). The organic material used in the present study were classified into two groups: MC, organic material formed in molecular clouds; and DC, organic material modified by exposure to ultraviolet radiation in diffuse clouds (Table 1). The chemical reagents for MC and DC were chosen based on laboratory analytical data (Greenberg and Mendoza-Gomez, 1991; Briggs et al., 1992; Greenberg et al., 2000).

Four different samples were used in the collision experiments as shown in Table 2. A molecular cloud organics (MC) sample without treatment, and molecular cloud and diffuse cloud organics (MC+DC) samples heated in a vacuum for 100 h at 333 K, 373 K, and 413 K. A rotary pump with a cold trap was used for evacuation. After heating the relevant samples in the vacuum chamber, the samples were pressed with a polytetrafluoroethylene (PTFE) sheet to obtain smooth surfaces.

Collision experiments

Head-on collision experiments were performed by allowing a copper sphere of 9.8 mm in diameter to free fall onto a copper block coated with organic matter. Figure 1 shows a schematic illustration of the apparatus. The vacuum chamber was evacuated to 10^{-2} Torr using a rotary pump with a cold trap. This setup resembles the ice-to-ice collision experiments of Higa et al. (1998). The holder for the copper sphere was located in the upper part of the vacuum chamber and fulfilled two roles: cooling and heating of the copper sphere, and release of the copper sphere. The target block was coated with 1 mm-thick organic matter and placed in the lower part of the vacuum chamber. The temperatures of the copper sphere and copper block were controlled at between 200 K and 410 K using liquid nitrogen and heaters.

The copper sphere was dropped on the inner surface of a funnel by rotating the holder

using a rotary manipulator. The copper sphere rolled and fell freely with an initial velocity of zero. The collision velocities were controlled at velocities slower than 7 m s^{-1} by changing the position of the funnel. A laser beam set above the copper block and an acoustic emission sensor attached to the copper block were employed to measure the collision velocity of the copper sphere. The error in velocity measurements was smaller than 0.01 m s^{-1}. The copper sphere was judged to have stuck to the organic matter based on the acoustic signal and video camera images. For the untreated sample, collision experiments were performed in a nitrogen atmosphere. Experiments for the other samples were conducted in a vacuum.

Measurements of viscoelastic properties

The dependence of the dynamic viscoelasticity of sample A on temperature was measured using a rheometer (RDS-II, Rheometric Scientific). The method of measurement has been described by Ferry (1980). The parallel plates method was adopted for measument as follows. The sample was placed between two plates, one of which was connected to a motor and the other to a transducer. When sinusoidal deformation was applied to the sample by the plate connected to the motor, the torque generated was measured by the transducer. This technique allows the dynamic shear modulus G' and dynamic shear viscosity η' to be obtained by analyzing the generated torque. Conditions of measurements are as follows: temperature, 125 to 303 K; thickness of parallel plate, 5.75 mm at T = 125-273 K and 25 mm at 288 and 303 K; angular frequency, 232 and 1.08 rad s^{-1}.

Measurements of tensile strength

The temperatures dependence of the tearing force between a copper sphere and an organic layer was measured using the experimental setup shown in Figure 2. In the present

study, the force at which the sphere began to separate from the sample layer was defined as the tearing force. A copper ball (9.8 mm in diameter) hung from a height gauge with 0.3-mm piano wire was brought into contact with the 1 mm-thick sample layer on the copper block. The copper block was connected firmly to the plate of an electronic balance. The contact area between the copper ball and the sample was several mm^2. The copper block was then cooled to 230-300 K with nitrogen gas, and sample and copper ball were exposed to a continuous flow of dry nitrogen to prevent frost formation. After the temperature of the copper ball had equalized to that of the sample, the copper ball was pulled up at a constant rate of 50 $\mu m\ s^{-1}$. The pulling force at the point when the organic layer began to tear from the copper block was recorded as the tearing force. Although the contact area between the copper ball and the sample immediately prior to tearing could not be determined accurately, the tearing force was confidently converted to a good approximation of tensile strength.

RESULTS

Collision experiments

Figure 3 shows the results of collision experiments between the copper sphere and the thin film of organic material. For sample A, complete sticking was observed at temperatures higher than 250 K, and the sticking threshold velocity, shown by a solid line, decreases with increasing temperature. At temperatures lower than 240 K, no sticking was observed. However, restitution coefficients are zero below the broken line. As a restitution coefficient of zero is considered to reflect sticking, the solid and broken lines represent the sticking velocity thresholds. The maximum sticking velocity is 5

m s^{-1} at around 250 K for sample A (Kouchi et al., 2002). For sample B (heated at 333 K), although the peak temperature increased to >320 K, the maximum sticking velocity was almo st the same as that of sample A.

For samples C and D, on the other hand, no sticking was observed at any of the temperatures measured. For sample C (heated at 373 K), the sticking threshold velocity decreased to 1 m s^{-1}, and was invariant with respect to temperature. Sample D (heated at 410 K) exhibited a similar tendency to sample C, with a sticking threshold velocity of 0.3 m s^{-1}. According to Kouchi et al. (2002), samples C and D are made of diffuse cloud organics (DC) only, and sample B molecular cloud organics and diffuse cloud organics. The relative stickiness of samples A and B is due to the stickiness of molecular cloud organics.

Viscoelastic properties

Figure 4 shows the temperature dependence of the dynamic shear modulus (G') and dynamic shear viscosity (η') for sample A. The dynamic shear modulus increases with decreasing temperature down to a constant at 200 K or below. No angular frequency (ω) dependence was observed. The dynamic shear viscosity (Fig. 4b) also increases with decreasing temperature, and becomes constant at 220 K or below. The values of η' for ω = 232 rad s^{-1} are three orders of magnitude smaller than those at ω = 1.08 rad s^{-1}, indicating that the sample has strong non-Newtonian fluid character over the entire temperature range measured. It is clear from Fig. 4 that sample A, consisting only of molecular cloud organics, is rigid at temperatures below 200 K and viscoelastic above 200 K. At around 300 K, the sample appears to be present in a liquid state.

Tensile strength

The temperature dependence of tearing force for sample A is shown in Fig. 5. As the adhesion force at the copper-organics interface was sufficiently strong to resist tearin g, tearing usually occurred at the deformed neck of the organic sample. The tearing force increased with decreasing temperature. If the neck diameter of the deformed sample is assumed to be constant (~2 mm^2) regardless of temperature, the tensile strengths are between 10^3 Nm^{-2} at 300 K and 10^6 Nm^{-2} at 230 K. The tearing force between the copper sphere and the organic layer after collisional sticking at 250 K was also measured, and the tensile strength was found to be 10^5 N m^{-2}, consistent with the other measurements.

DISCUSSION

Mechanism of sticking and repulsion

At temperatures between 200 and 220 K (region L in Fig. 3a), MC organics form a rigid body as clarified by the viscoelastic measurements (Fig. 4). It is clear that the collision of organics-coated silicate grains in this temperature range (region L in Fig. 6) is a collision between rigid bodies. Therefore, repulsion is observed in region L.

At temperatures higher than 290 K (region H in Fig. 3a), the viscosity of the MC organics becomes low. When a collision between organics-coated silicate grains occurs at these temperatures, the organic matter is easily deformed and the silicate grains collide without loss of kinetic energy (region H, Fig. 6). Furthermore, the tearing force is very low in this region (Fig. 5). These factors result in the repulsion observed in region H.

At temperatures around 250 K, the MC organics act as both an elastic (or rigid) and plastic body, and can be considered to be a viscoelastic material. During the collision of organic layers at relatively low temperatures, a large amount of kinetic energy is dissipated by the deformation or flow of organic matter. This results in the tendency of the colliding particles to stick before the silicate cores c ome into contact. Although the silicate cores did collide at relatively high temperatures, the dissipation of kinetic energy during the rebound also promotes sticking. At collisional velocities higher than 5 m s^{-1}, the rebound velocity is sufficient to break the organic layer at all temperatures examined.

The stickiness of organic material compared to silicates and ices is considered to be explainable as follows. At temperatures higher than 220 K, the organic material is viscoelastic, and as such may act as a liquid bridge that holds the two grains together. The sticking force between particles by this liquid bridge (Erle et al., 1971) is an order of magnitude greater than that due to van der Waals force (Chokshi et al., 1993). However, this liquid-bridge force is still not sufficient to explain the observed stickiness of organic matter. The viscoelastic behavior during collision and the kinetic energy dissipation as a result of deformation or flow of organic matter

are considered to reduce the rebound velocity of the sphere as already discussed. After reducti on of the rebound velocity, the liquid-bridge force then becomes sufficient to hold the sphere. Therefore, this combination of mechanisms is considered to be the origin of the strong stickiness of this organic material.

Distribution of planetary materials

To discuss the distribution of planetary materials in the protosolar nebula based

on the results of heating experiments, Kouchi et al. (2002) employed an accretion disk model developed by Bell et al. (1997) and assumed a mass accretion rate of the disk of 10^{-7} solar mass/yr with $\alpha = 0.004$. Kouchi et al. (2002) concluded that most interstellar organic material evaporated at heliocentric distance of 2.2 AU from the center of the protosolar nebula, that diffuse cloud organics existed between 2.2 and 2.6 AU, and that molecular cloud organics coexisted with diffuse cloud organics at >2.6 AU during the accretion disk stage. Kouchi et al. (2002) also showed that the stickiest condition was between 2.6 AU and 3.8 AU based on the experimental results in Fig. 3a of the present paper. It should be noted that the heliocentric distances determined in this way depend heavily on the accretion model itself and the parameters used. Furthermore, interstellar grains are assumed to enter the solar nebula without alteration and the properties of organic materials are assumed to be determined solely by local temperature. Although these assumptions may not be accurate, the discussion is valuable assuming the most extreme case.

In the present paper, an empirical temperature distribution of 500 K at 2 AU and 250 K at 3 AU is employed for the accretion disk instead of the above model because if the temperature at 3 AU is higher, achondrites must have formed at >3 AU according to the peak range of organic material stickiness (discussed in the next section). However, as a number of C-type asteroids similar to carbonaceous chondrites are known to formed at around 3 AU (Bell et al., 1989), the temperature at 3 AU is considered to be 250 K. Furthermore, Nakano et al. (2002) suggested that ordinary and enstatite chondrites should have formed at around 2-2.2 AU based on analysis of the redox state of the solar nebula, indicating that the temperature at 2 AU should be about 500 K. This is also supported by the formation of E- and S-type asteroids, which are similar to enstatite and ordinary chondrites, in this region.

Figure 7 shows the distribution of planetary material during evolution from the accretion disk to a passive disk. As most of the interstellar organic material is evaporates at 2.1 AU, only silicate minerals remain at <2.1 AU. The vertical boundary between the silicates and organic material can be explained as due to the evaporative thermal decomposition of organic material (Nakano et al., 2002), which could not recondense when the protosolar nebula cooled to form the passive disk. Ice crystals on the other hand recondense at temperatures low er than about 160 K (>3.0 AU). The major difference between the results in Kouchi et al. (2002) and those in the present study is difference in the range of greatest stickiness, 2.3-3.0 AU in the present case compared to 2.6-3.8 AU. This is very important in terms of the range of formation of achondrite parent bodies, as will be discussed later.

Formation of planetesimals

In collision experiments using millimeter-size silicate and ice grains, sticking has not been observed even at lower collision velocities, 0.15 m s^{-1} for silicate (Hartmann, 1978; Blum and Muench, 1993) and 0.15×10^{-3} m s^{-1} for ice (Bridges et al., 1984; Hatzes et al., 1988; Higa et al., 1998), while sticking has been observed for micrometer-size silicate particles (Wurm and Blum, 1998; Poppe et al., 2000). The present experimental results clearly show that organic matter is stickier in the coagulation of millimeter-size grains than silicate or ice, and that the coagulation of organic grains can occur even at collision velocities on the order of m s^{-1}. Therefore, these results suggest that millimeter-size organic grain aggregates are likely to have stuck together to form larger aggregates, even during the turbulent stage of the protosolar nebula, as proposed by Weidenschilling and Cuzzi (1993). The growth of grain aggregates without organic mantles is possible through the dissipation of internal energy (e.g., Dominik and Tielens, 1997; Sirono, 1999). In the case of organic-coated grain aggregates, internal energy dissipation is also affected

by the viscoelastic properties of the organic material as discussed above.

Figure 7 also shows the range of greatest stickiness for organic material determined through the collision experiments (Figs. 3a-d). At 2.3-3.0 AU, grains pass through the region of decreasing nebula temperature and coagulate. The coagulation of grain aggregates, and the formation of planetesimals, therefore is considered to have occurred more rapidly in asteroid belts than in terrestrial or Jovian regions.

Formation of small bodies in asteroid belts

Why are only very small bodies, rather than planet-sized objects, formed in asteroid belts? Asteroids have conventionally been considered to be the product of the fragmentation and destruction of comparatively large protoplanets (Wetherill, 1989). However, Kouchi et al. (2002) proposed a very different and new idea on the basis of collision experiments (Fig. 7, Table 3). As has already been shown, the coagulation of grain aggregates occurs very rapidly in an asteroid belt due to the stickiness of organic matter despite the turbulent conditions (Fig. 8b, c). The formation of planetesimals is expected from such coagulation of grain aggregates, as shown by Weidenschilling and Cuzzi (1993). During the formation of planetesimals, aggregates of around 1 m in size rapidly decelerate and fall due to the strong gas drag (Adachi et al., 1976). As a result, the source materials for asteroids rapidly become scarce in the region 2.3-3.0 AU. Therefore, asteroids in general will not grow to significant sizes because potential planetesimals are remove from the coagulatory system due to gas drag, and not because of fragmentation as previously suggested (Wetherill, 1989). Collisional fragmentation of asteroids is still possible as a result of gravitational perturbation after the formation of Jupiter. At that time, the fundamental

structure of the asteroid belt had already been formed. It can also be concluded from this argument that asteroids are the oldest bodies in the solar system.

The large amount of material supplied from the asteroid belt to regions around terrestrial planets is an important factor in the formation and composition of the terrestrial planets.

Asteroids formed in the region 2.3-3.0 AU might be equivalent to achondrite parent bodies. These parent bodies grow in the accretion disk in the presence of abundant ^{26}Al (Table 3), resulting in melting and differentiation. On the other hand, silicate grains at <2.1 AU and icy grains at >3.0 AU do not stick together to form aggregates in a turbulent accretion disk because of the very small sticking threshold velocity of these materials. The formation of planetesimals at <2.1 AU and >3.0 AU occurs in the static passive disk stage. These parent bodies did not melt because of insufficient remaining ^{26}Al. Instead of melting, thermal metamorphism at <2.1 AU and aqueous alteration at >3.0 AU are considered to have occurred.

Acknowledgments

The authors thank J. M. Greenberg, W. F. Huebner, and A. Cellino for discussions and critical comments and D. Brownlee, M. Kress, and C. Dominik for constructive reviews. H. Yano, S. Sirono, K. Kuramoto, and H. Yurimoto are also acknowledged for helpful discussions. This work was supported in part by a Grant-in-Aid for scientific research from the Japan Society for the Promotion of Science.

REFERENCES

ADACHI I., HAYASHI C. AND NAKAZAWA K. (1976) The gas drag effect on the elliptic motion of a solid body in the primordial solar nebula. *Prog. Theor. Phys.* **56**, 1756-1771.

BELL K. R., CASSEN P. M., KLAHR H. H. AND HENNING TH. (1997) The structure and

appearance of protostellar accretion disks: Limits on disk flaring. *Astrophys. J.* **486**, 372-387.

BELL J. F., DAVIS D. R., HARTMANN W. K. AND GAFFEY M. J. (1989) Asteroids: the big picture. In *Asteroids II* (eds. Binzel, R. P., Gehrels T. and Matthews M. S.), pp. 921-945. Univ. of Arizona Press, Tucson, Arizona, U.S.A.

BLUM J. AND MUENCH M. (1993) Experimental investigation on aggregate-aggregate collisions in the early solar nebula. *Icarus* **106**, 151-167.

BRIDGES F. G., HATZES A. P. AND LIN D. N. C. (1984) Structure, stability and evolution of Saturn's rings. *Nature* **309**, 333-335.

BRIGGS R., ERTEM G., FERRIS J. P., GREENBERG J. M., MCCAIN P .J., MENDOZA-GOMEZ C. X. AND SCHUTTE W. (1992) Comet Halley as an aggregate of interstellar dust and further evidence for the photochemical formation of organics in the interstellar medium. *Origins Life Evol. Biosphere* **22**, 287-307.

BAR-NUN A., HERMAN G., LAUFER D. AND RAPPAPORT M. L. (1995) Trapping and release of gases by water ice and implications for icy bodies. *Icarus* **63**, 317-332.

CHOKSHI A., TIELENS A. G. G. M. AND HOLLENBACH D. (1993) Dust coagulation. *Astrophys. J.* **407**, 806-819.

DOMINIK C. AND TIELENS A. G. G. M. (1997) The physics of dust coagulation and the structure of dust aggregates in space. *Astrophys. J.* **480**, 647-673.

FERRY J. D. (1980) *Viscoelastic Properties of Polymers, 3rd Ed.*, John Wiley & Sons, New York.

GREENBERG J. M. (1998) Making a comet nucleus. *Astron. Astrophys.* **330**, 375-380.

GREENBERG J. M. AND MENDOZA-GOMEZ C. X. (1991) Interstellar dust evolution: A reservoir of prebiotic molecules. In *The Chemistry of Life's Origins* (eds. Greenberg J. M., Mendoza-Gomez C. X. and Pirronello V.), pp.

1-32. Kluwer, Dordrecht, the Netherlands.

GREENBERG J. M., GILLETTE J. S, CARO G. M. M., MAHAJAN T. B., ZARE R. N., LI A., SCHUTTE W. A., GROOT M. AND MENDOZA-GOMEZ C. X. (2000) Ultraviolet photoprocessing of interstellar dust mantles as a source of polycyclic aromatic hydrocarbons and other conjugated molecules. *Astrophys. J.* **531**, L71-73.

GREENBERG J. M. AND LI A. (1996) What are the true astronomical silicates? *Astron. Astrophys.* **309**, 258-266.

HARTMANN W. K. (1978) Planet formation: mechanism of early growth. *Icarus* **33**, 50-61.

HASHIMOTO A., KUMAZAWA M. AND ONUMA N. (1979) Evaporation metamorphism of primitive dust material in the early solar nebula. *Earth Plant. Sci. Lett.* **43**, 13-21.

HAYASHI C., NAKAZAWA K. AND NAKAGAWA Y. (1985) Formation of the solar system. In *Protostars and Planets II* (eds. Black D. C. and Matthews M. S.), pp. 1100-1153. Univ. of Arizona Press, Tucson, Arizona, USA.

HATZES A. P., BRIDGES F. G. AND LIN D. N. C. (1988) Collosional properties of ice spheres at low impact velocities. *Mon. Not. Roy. Astron. Soc.* **231**, 1091-1115.

HIGA M., ARAKAWA M. AND MAENO N. (1998) Size dependence of restitution coefficients of ice in relation to collision strength. *Icarus* **133**, 310-320.

KOUCHI A. (1990) Evaporation of H_2O-CO ice and its astrophysical implications. *J. Cryst. Growth* **99**, 1220-1226.

KOUCHI A., KUDO T., NAKANO H., ARAKAWA M., WATANABE N., SIRONO S., HIGA M. AND MAENO N. (2002) Rapid growth of asteroids owing to very sticky interstellar organic grains. *Astrophys. J.* **566**, L121-L124.

NAKANO H., KOUCHI A., TACHIBANA S. AND TSUCHIYAMA A. (2002) Evaporation of interstellar organic materials in the solar nebula. *Astrophys. J.* (submitted)

POPPE T., BLUM J. AND HENNING T. H. (2000) Analogous experiments on the stickiness of micron-sized preplanetary dust. *Astrophys. J.* **533**, 454-471.

SIRONO S. (1999) Effects by sintering on the energy dissipation efficiency in collisions of grain aggregates. *Astron. Astrophys.* **347**, 720-723.

WEIDENSCHILLING S. J. AND CUZZI J. N. (1993) Formation of planetesimals in the solar nebula. In *Protostars and Planets III* (eds. Levy E. H. and Lunime J. I.), pp. 1031-1060.Univ. of Arizona Press, Tucson, Arizona, U.S.A.

WETHERILL G. W. (1989) Origin of the asteroid belt. In *Asteroids II* (eds. Binzel, R.P., Gehrels T. and Matthews M. S.), pp. 661-680. Univ. of Arizona Press, Tucson, Arizona, USA.

WURM G. AND BLUM J. (1998) Experiments on preplanetary dust aggregation. *Icarus* **132**, 125-136.

Figure captions

Fig. 1. Schematic illustration of setup for collision experiments

Fig. 2. Schematic illustration of experimental setup for measurement of tearing force

Fig. 3. Conditions for sticking and repulsion for collision of a copper sphere onto an analogue of an interstellar organic material layer; (a) sample A, (b) sample B heated at 333 K, (c) sample C heated at 373 K, and (d) sample D heated at 413 K. Solid circles and crosses represent sticking and repulsion, respectively. Open triangles indicate no observed sticking but restitution coefficient of zero, solid and

broken lines represent the sticking threshold velocities of an interstellar organic matter analogue. L, M, and H denote regions where the mechanism of sticking and repulsion differs as discussed in Fig. 6.

Fig. 4 Temperature dependence of (a) dymanic shear modulus and (b) and dynamic viscosity of sample A

Fig. 5 Temperature dependence of tearing force between a copper sphere and an organic layer (sample A). Error bars represent statistical error.

Fig. 6 Schematic illustration of the mechanism of sticking and repulsion for organics-coated silicate grains in three different regions corresponding to those in Fig. 3a.

Fig. 7. Diagram showing the occurrence of grain surface materials, silicates, molecular cloud (MC) and diffuse cloud (DC) organic matter, and ice, during evolution from an accretion disk to a passive disk. The structures of grains in the respective regions are also shown: brown, silicates; grey, diffuse cloud organic material; yellow, molecular cloud organic material; blue, ice. The red line shows the temperature distribution of the accretion disk (see text for details) and the blue line the passive disk (Hayashi et al., 1985). The region of sticking threshold velocities greater than 2.0 m s^{-1} is shown by the green line, and the arrow indicates the cooling history of the grain aggregates.

Fig. 8. Schematic illustration of the evolution of asteroids. (a) and (b) represent the final stage of a turbulent accretion disk, and (c) and (d) represent a passive disk. The faint color regions indicate the existence of grains corresponding to Fig. 7. The formation

of planetesimals at 2.3-3.0 AU occurs in stage (b) due to the sticking effect of organic grains. During the formation of these planetesimals, most of the material in this region (1 m in size) fall due to gas drag. The growth of the planetesimals ceases in stage (c) due to the lack of raw materials. These bodies become achondrite parent bodies. The falling material at 2.3-3.0 AU grow to 100 m in size during the fall and forms the supply of material for the region of terrestrial planets. The formation of planetesimals at <2.3 and >3.0 AU occurs in stage (d).

TABLE 1 Composition of an interstellar organic matter analogue. MC: molecular cloud organic matter; and DC: diffuse cloud organic matter.

chemical compounds	chemical formulae	wt %
MC acetamide	CH_3CONH_2	4.1
urea	H_2NCONH_2	0.5
ethylene glycol	$HOCH_2CH_2OH$	1.2
glycolic acid	$HOCH_2COOH$	7.2
lactamide	$CH_3CH(OH)CONH_2$	5.4
glycerol	$HOCH_2CH(OH)CH_2OH$	1.4
hexamethylene tetramine	$C_6H_{12}N_4$	0.7
indene	C_9H_8	4.7
1,2-dimethylnaphthalene	$C_{10}H_6(CH_3)_2$	1.6
1,4-diisopropenylbenzene	$C_6H_4[C(CH_3)CH_2]_2$	2.0
cyclohexyl phenyl ketone	$C_6H_{11}COC_6H_5$	5.0
4'-cyclohexylacetophenone	$C_6H_{11}C_6H_4COCH_3$	4.4
4-(1-adamantyl)phenol	$C_{10}H_{15}C_6H_4OH$	1.3
4,4'-methylenebis(2,6-dimethylphenol)	$C_{17}H_{20}O_2$	1.4
α,α'-bis(4-hydroxyphenyl)-1,4-diisopropylbenzene	$HOC_6H_4C(CH_3)_2C_6H_4C(CH_3)_2C_6H_4OH$	0.1
phenanthrene	$C_{14}H_{10}$	6.8
lauric acid	$CH_3(CH_2)_{10}COOH$	3.8
sebacic acid	$HOOC(CH_2)_8COOH$	3.9
eicosanoic acid	$CH_3(CH_2)_{18}COOH$	6.0
DC phenanthrene	$C_{14}H_{10}$	5.2
pyrene	$C_{16}H_{10}$	4.3
benzopyrene	$C_{20}H_{12}$	6.7
benzoperylene	$C_{22}H_{12}$	3.9
coronene	$C_{24}H_{12}$	18.4

TABLE 2 Preparation of samples for collision experiments

Name	Starting materials	Heating temperature	Heating duration
Sample A)	MC		
Sample B)	MC + DC	333 K	100 hours
Sample C)	MC + DC	373 K	100 hours
Sample D)	MC + DC	413 K	100 hours

TABLE 3. Evolution of meteorites' parent bodies

	<2.1 AU	2.3-3.0 AU	>3.0 AU
Grain surface material	Silicate	molecular cloud organics	Molecular cloud organics to ice
V_{crit}[a]	Very small	5 m/s	Very small
Formation of planetesimals	Passive disk	Accretion disk	Passive disk
Amount of ^{26}Al	Small	Large	Small
Evolution	Thermal metamorphism	Melting and differentiation	Aqueous alteration

a) Maximum value of the sticking threshold velocity.

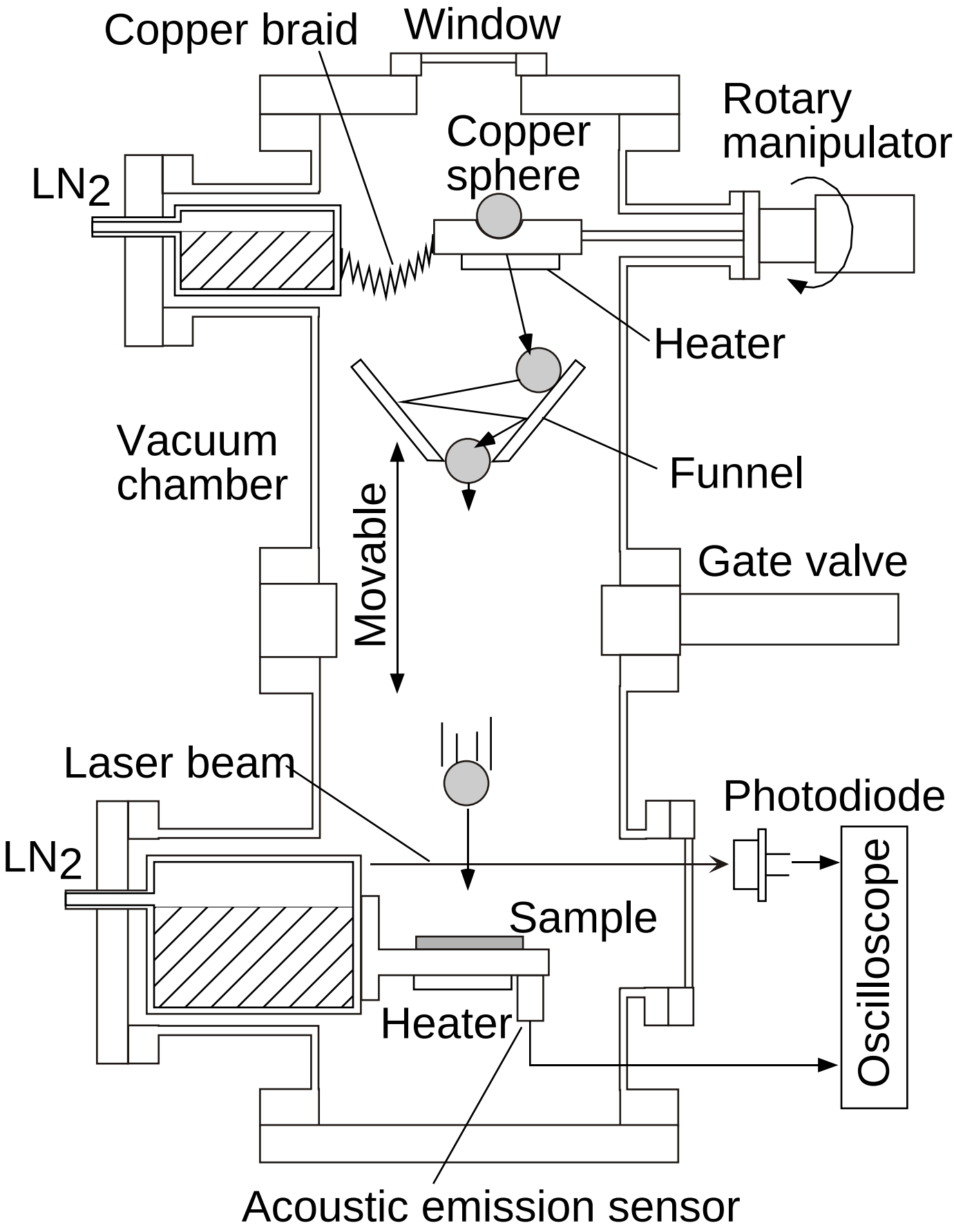
Copper braid
Window
Rotary manipulator
Copper sphere
LN2
Heater
Vacuum chamber
Funnel
Movable
Gate valve
Laser beam
Photodiode
LN2
Sample
Heater
Oscilloscope
Acoustic emission sensor

Kouchi Fig. 1

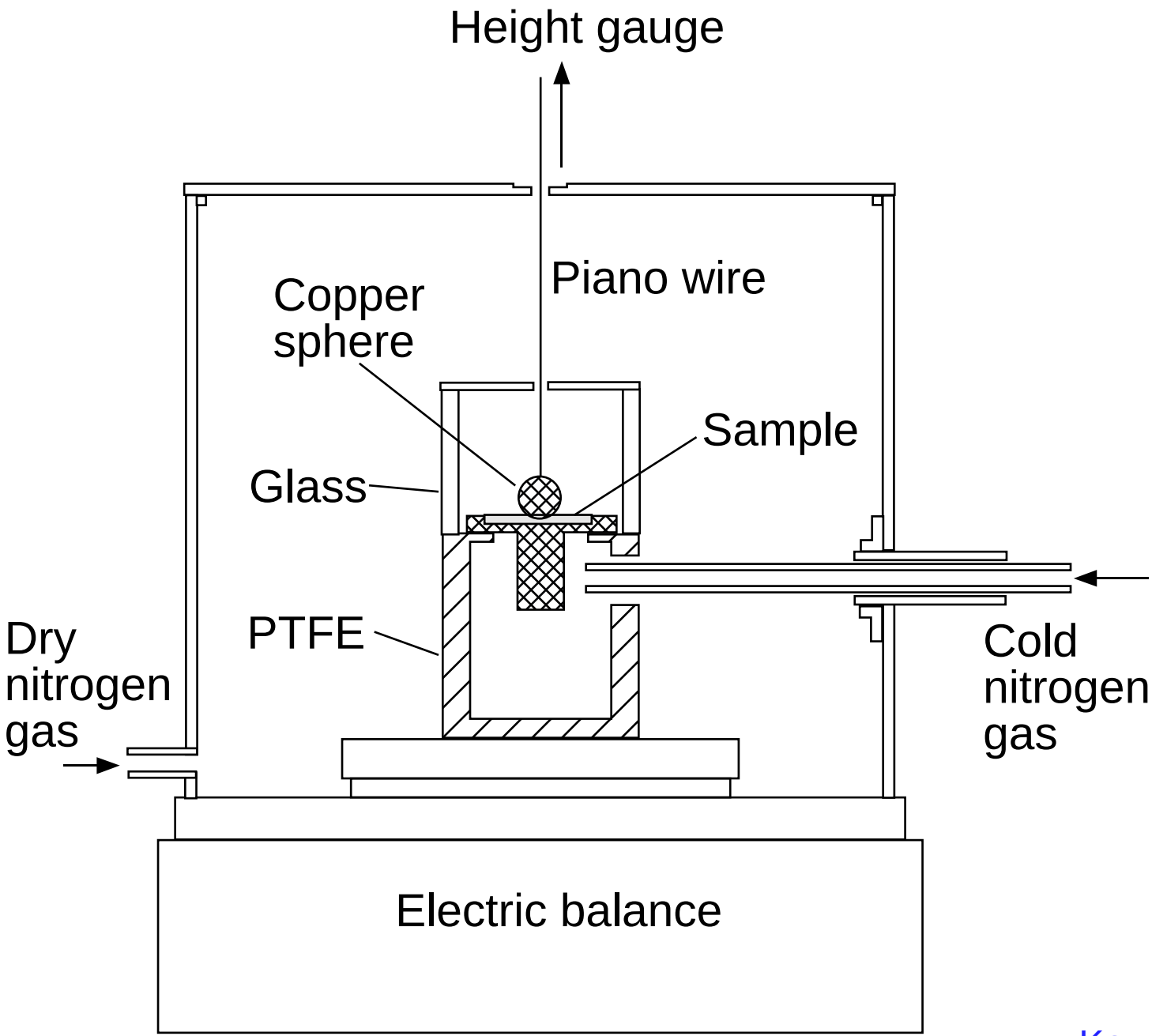
Height gauge
Piano wire
Copper sphere
Sample
Glass
PTFE
Dry nitrogen gas
Cold nitrogen gas
Electric balance

Kouchi Fig.2

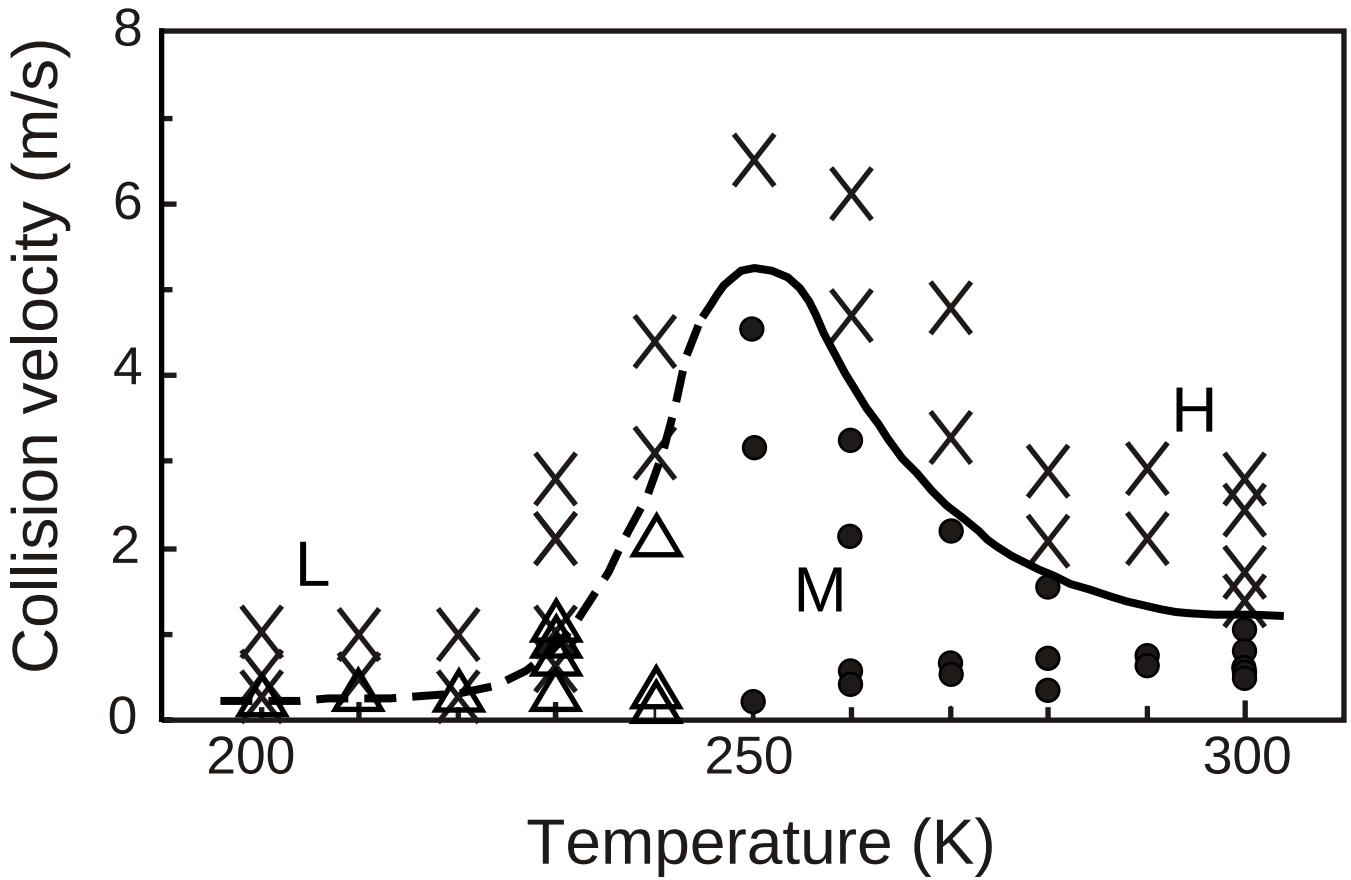

Kouchi Fig. 3a

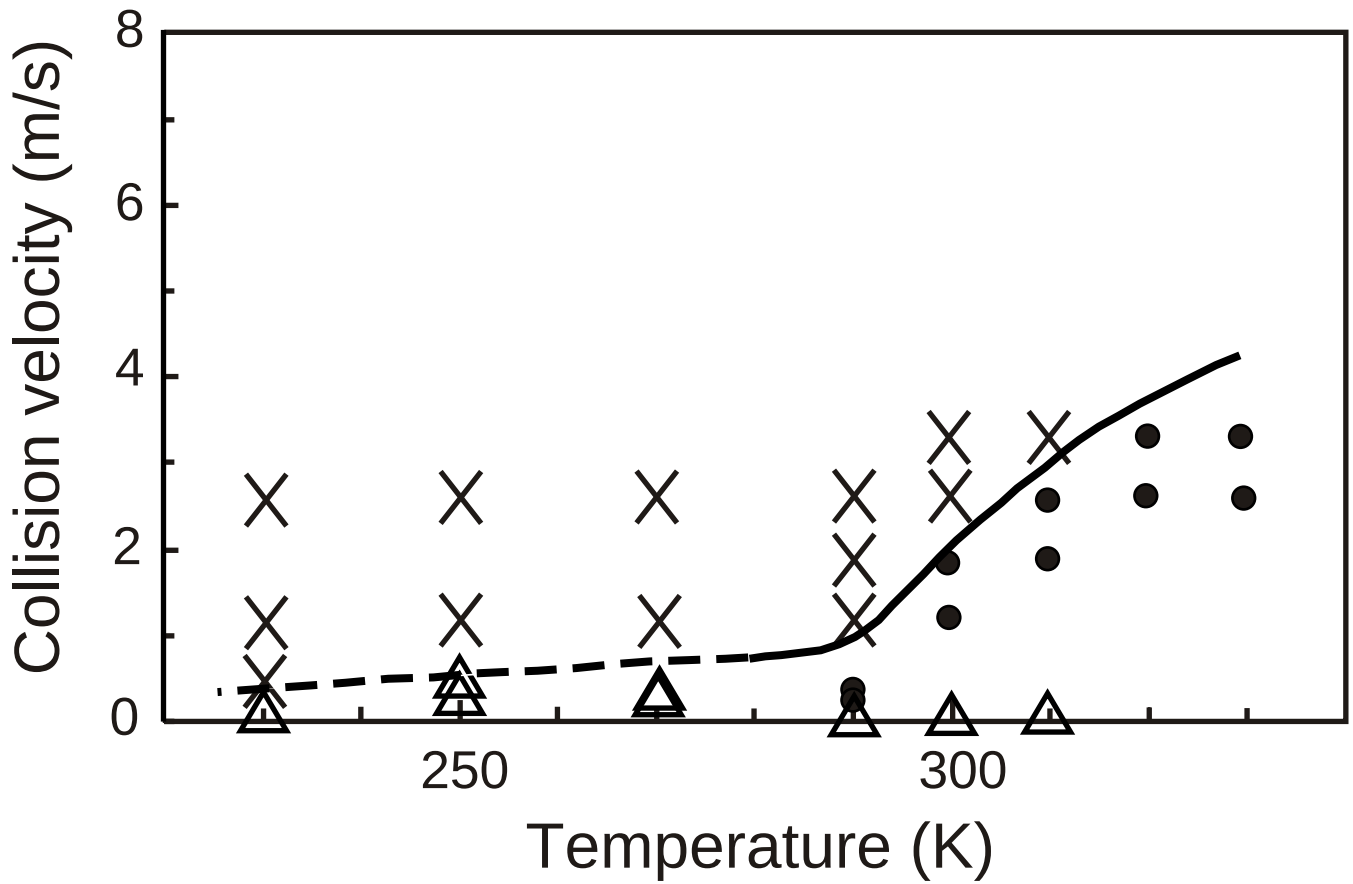

Kouchi Fig. 3b

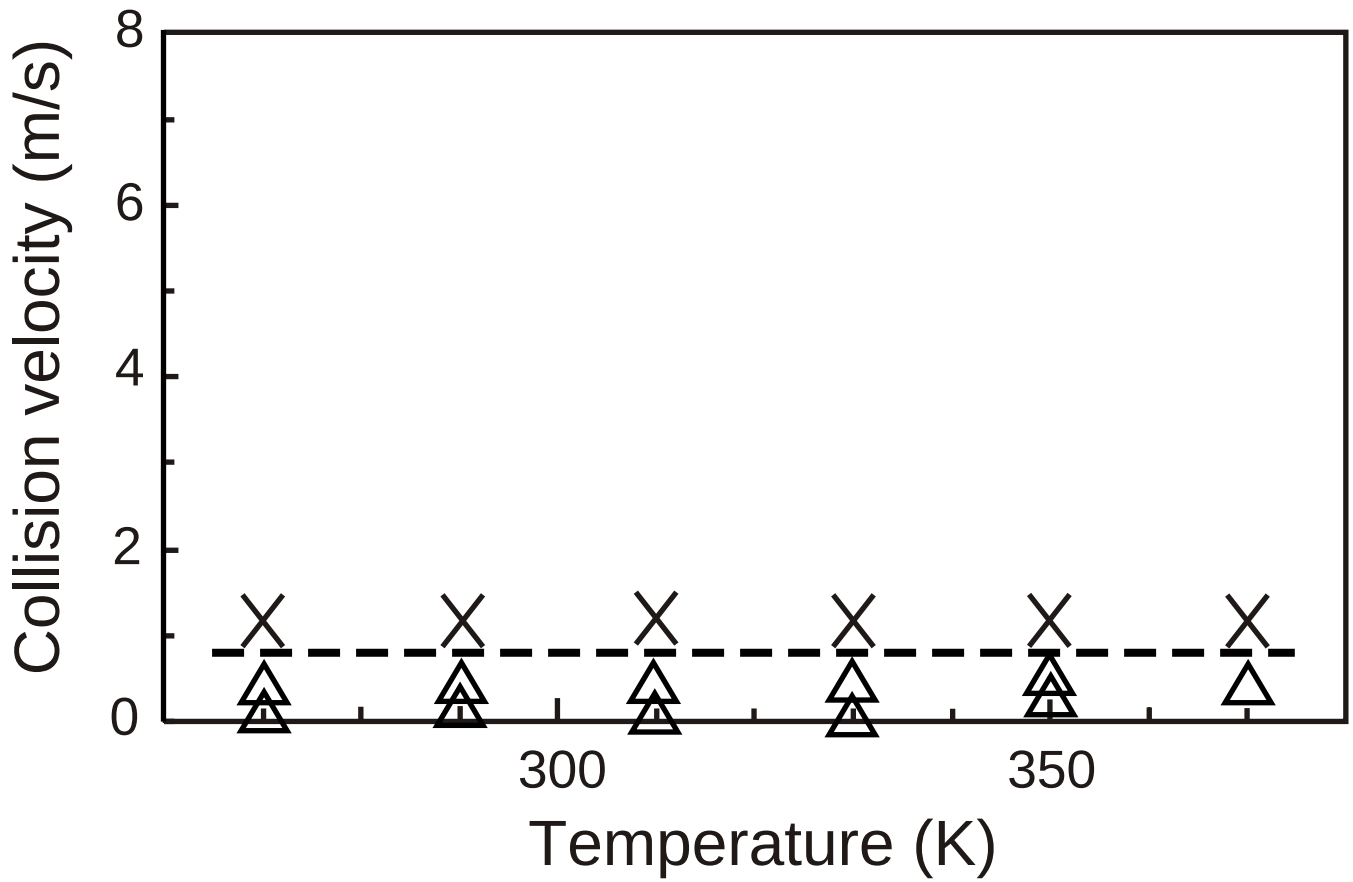

Kouchi Fig. 3c

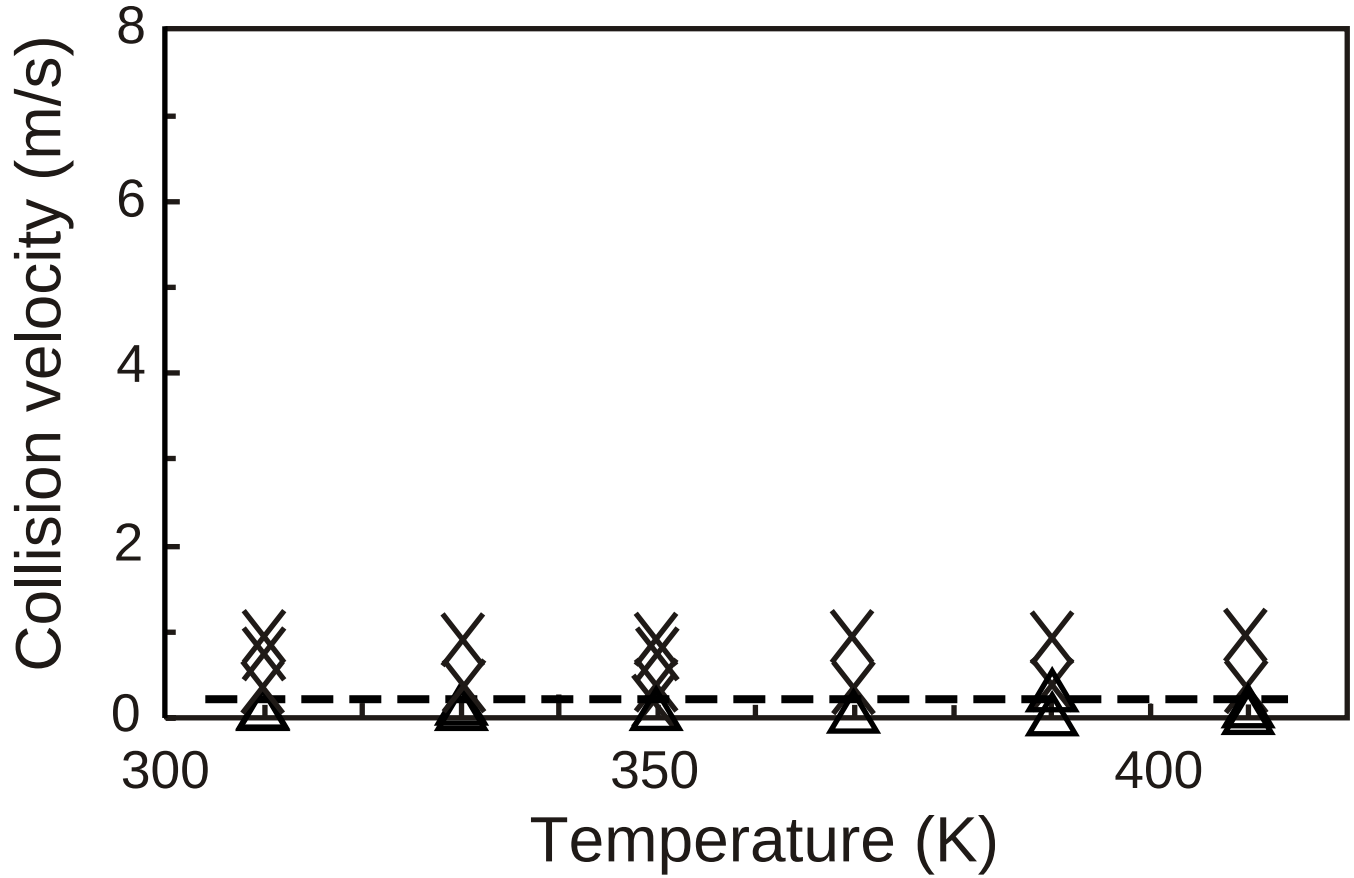

Kouchi Fig. 3d

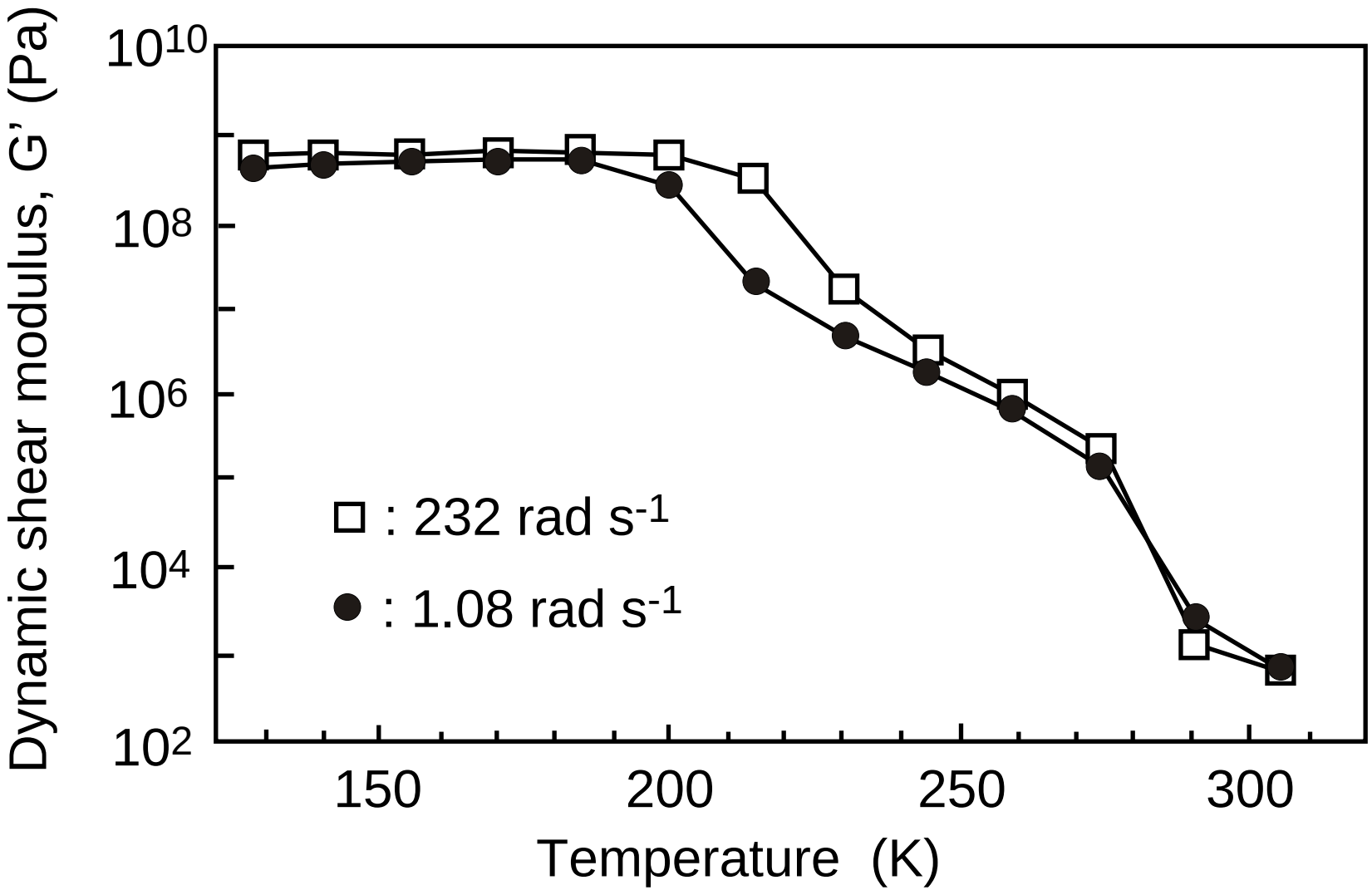

Kouchi Fig. 4a

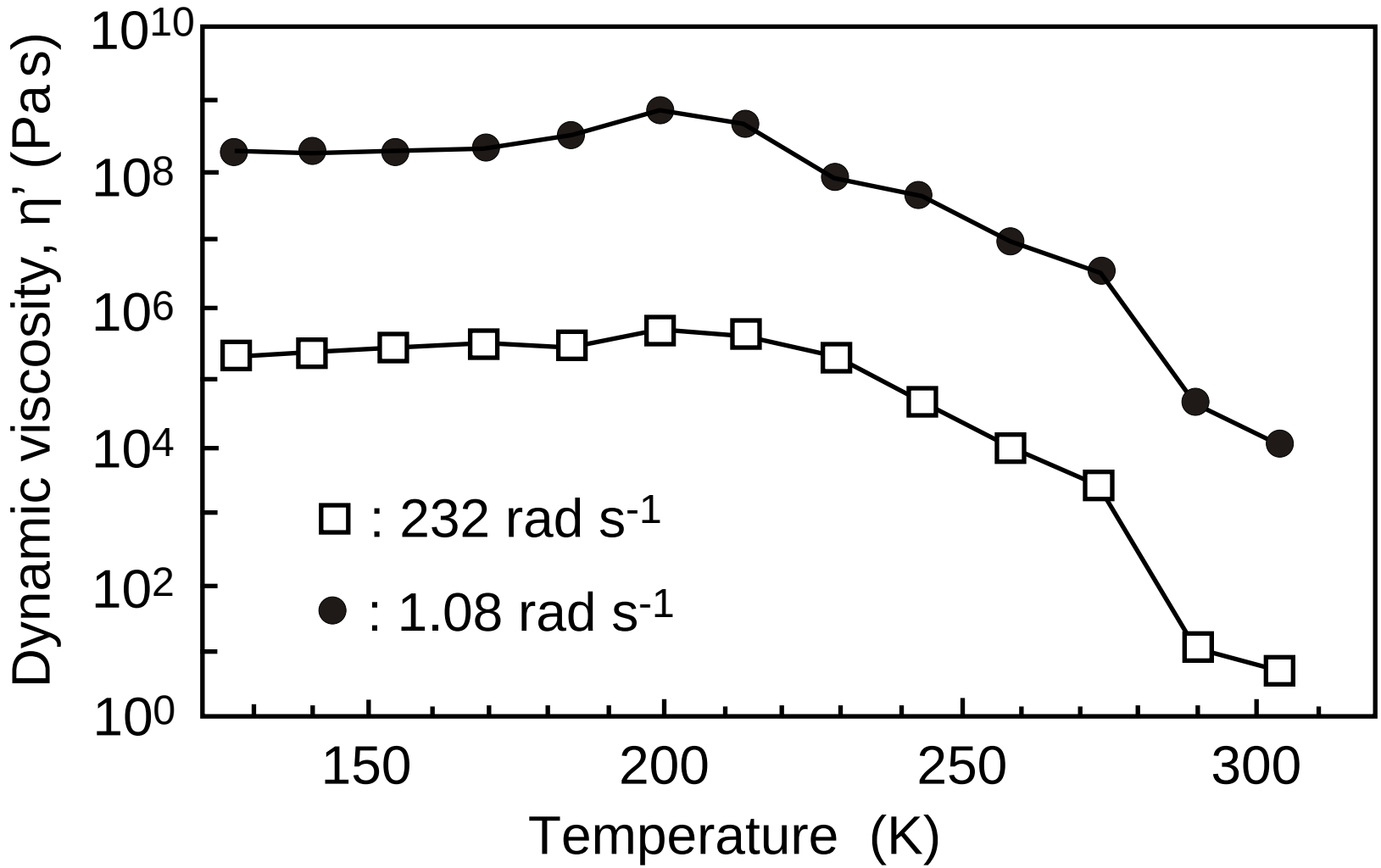

Kouchi Fig. 4b

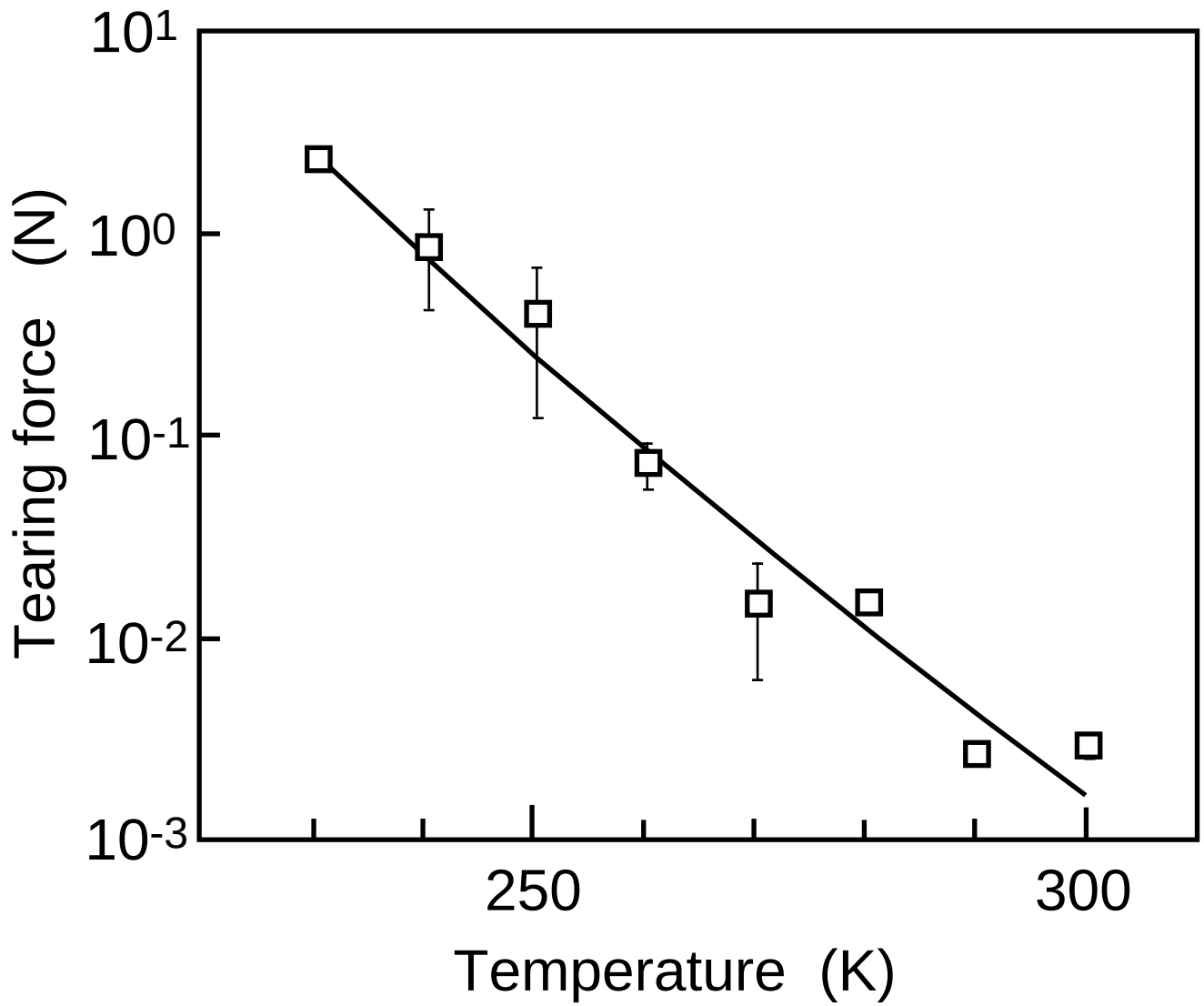

Kouchi Fig. 5

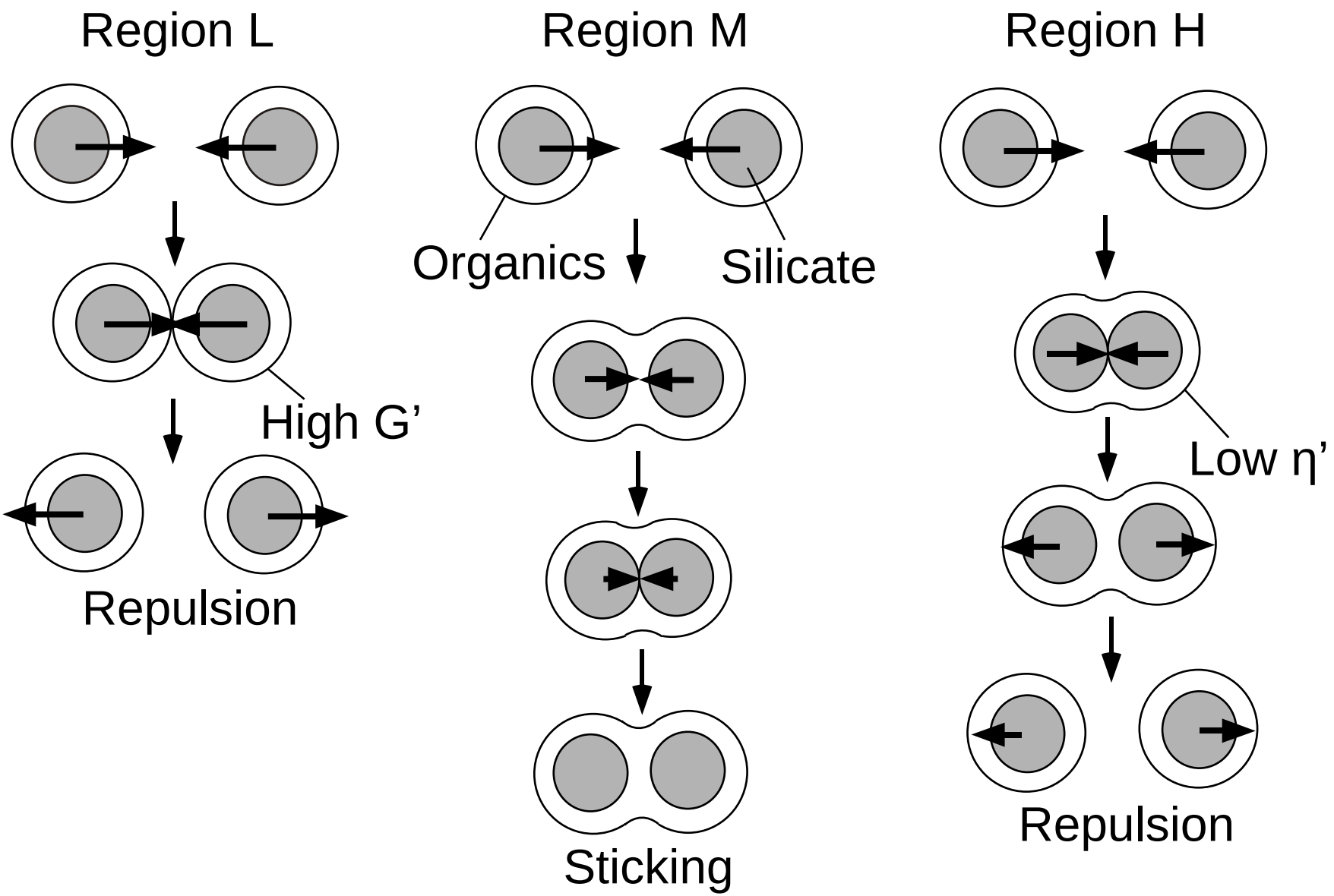
Region L
Region M
Region H
Organics
Silicate
High G'
Low η'
Repulsion
Sticking
Repulsion

Kouchi Fig. 6

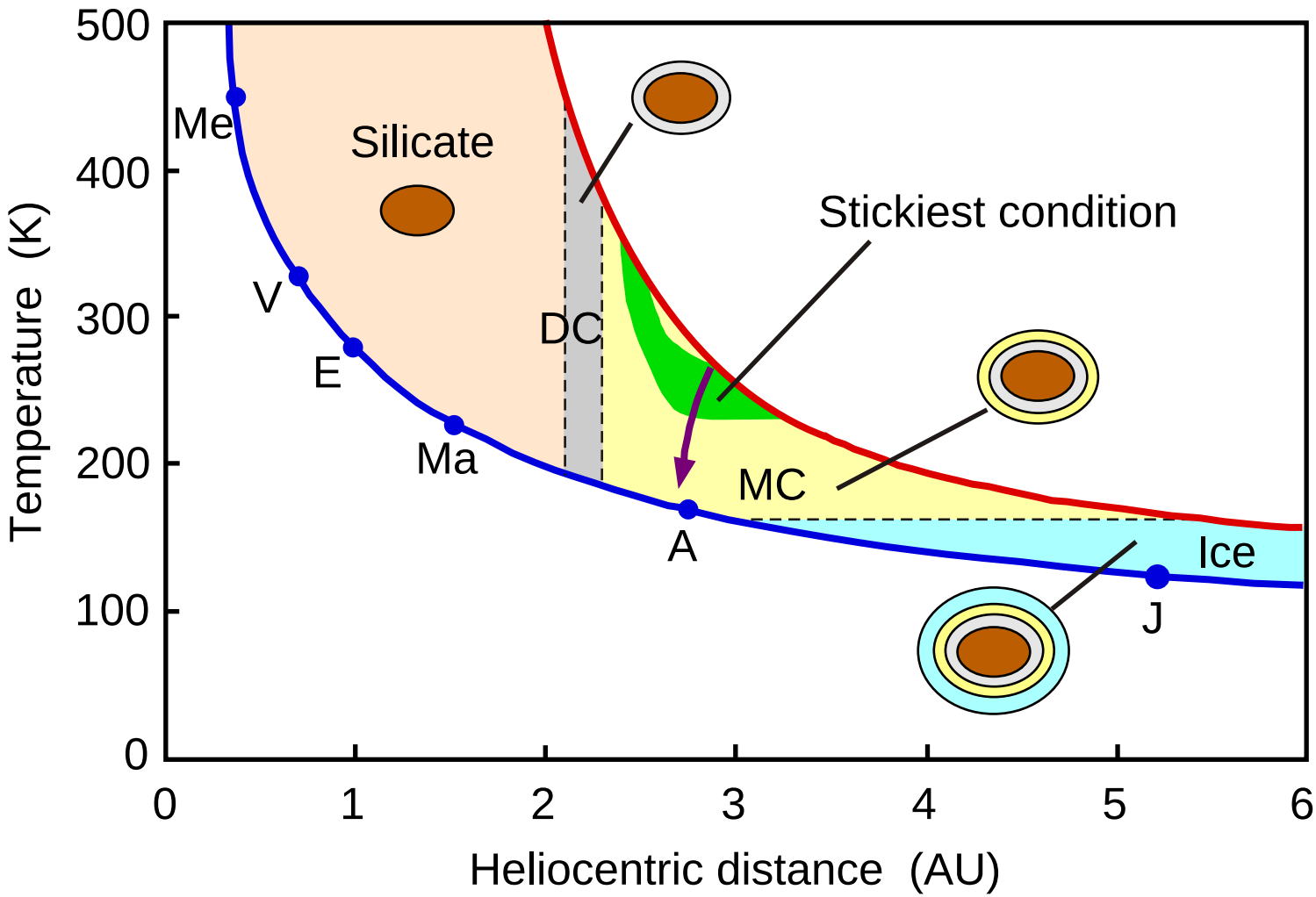
500
400
300
200
100
0
Temperature (K)
0
1
2
3
4
5
6
Heliocentric distance (AU)
Me
V
E
Ma
A
J
Silicate
DC
Stickiest condition
MC
Ice

Kouchi Fig. 7

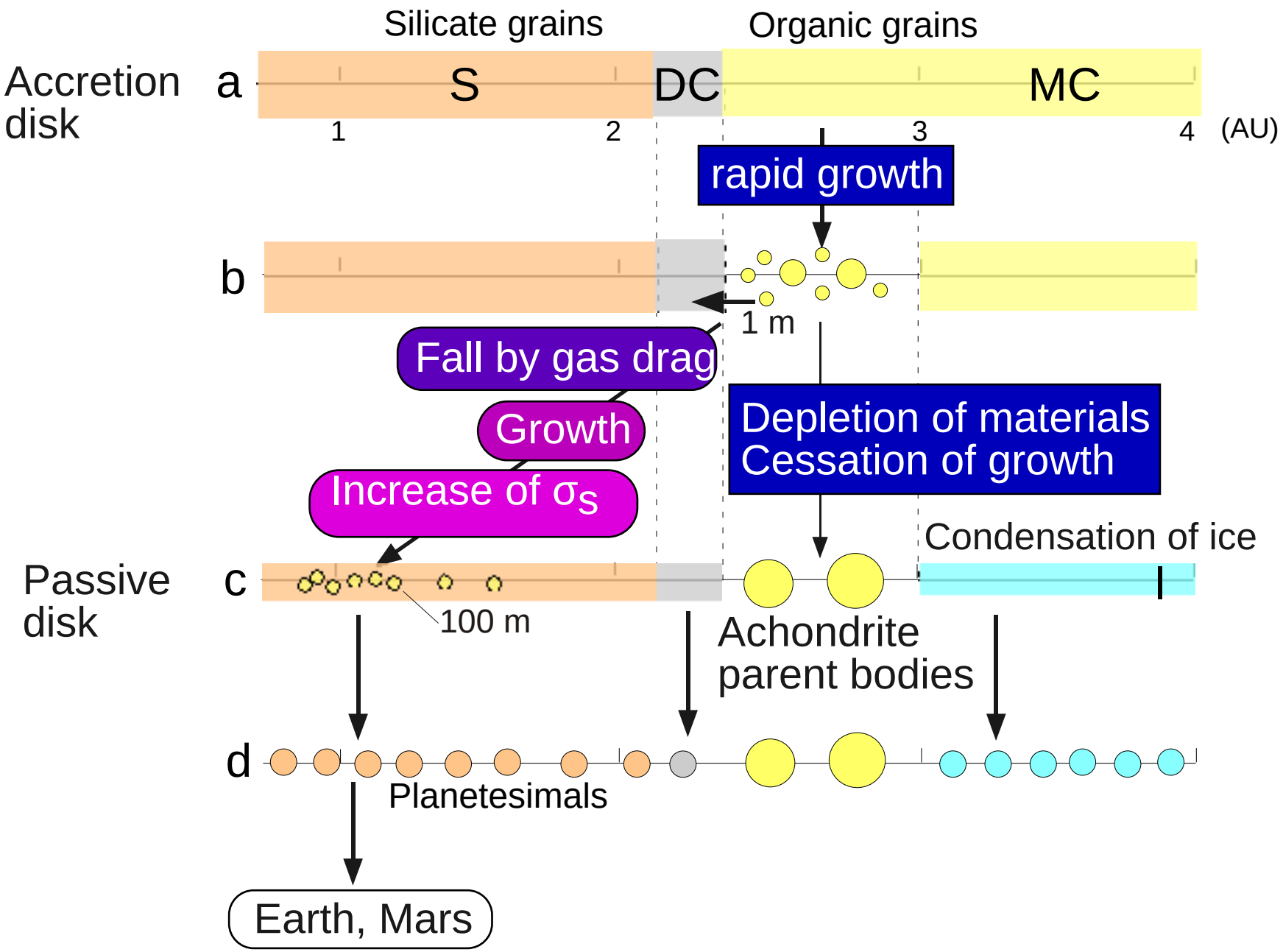
Silicate grains
Organic grains
Accretion disk
a
S
DC
MC
1
2
3
4
(AU)
rapid growth
b
1 m
Fall by gas drag
Growth
Increase of σS
Depletion of materials
Cessation of growth
Condensation of ice
Passive disk
c
100 m
Achondrite parent bodies
d
Planetesimals
Earth, Mars

Kouchi Fig. 8